HHS Public Access

Author manuscript

J Neurooncol. Author manuscript; available in PMC 2016 January 25.

Published in final edited form as:

J Neurooncol. 2015 October ; 125(1): 149–156. doi:10.1007/s11060-015-1881-3.

Long-term risk of radionecrosis and imaging changes after stereotactic radiosurgery for brain metastases

Zachary A. Kohutek[1], **Yoshiya Yamada**[1], **Timothy A. Chan**[1,2], **Cameron W. Brennan**[2,3], **Viviane Tabar**[3], **Philip H. Gutin**[3], **T. Jonathan Yang**[1], **Marc K. Rosenblum**[4], **Åse Ballangrud**[5], **Robert J. Young**[6], **Zhigang Zhang**[7], and **Kathryn Beal**[1]

Kathryn Beal: bealk@mskcc.org

[1]Department of Radiation Oncology, Memorial Sloan Kettering Cancer Center, 1275 York Ave., New York, NY 10065, USA

[2]Human Oncology and Pathogenesis Program, Memorial Sloan Kettering Cancer Center, New York, NY, USA

[3]Department of Neurosurgery, Memorial Sloan Kettering Cancer Center, New York, NY, USA

[4]Department of Pathology, Memorial Sloan Kettering Cancer Center, New York, NY, USA

[5]Department of Medical Physics, Memorial Sloan Kettering Cancer Center, New York, NY, USA

[6]Department of Radiology, Memorial Sloan Kettering Cancer Center, New York, NY, USA

[7]Department of Epidemiology and Biostatistics, Memorial Sloan Kettering Cancer Center, New York, NY, USA

Abstract

Radionecrosis is a well-characterized effect of stereotactic radiosurgery (SRS) and is occasionally associated with serious neurologic sequelae. Here, we investigated the incidence of and clinical variables associated with the development of radionecrosis and related radiographic changes after SRS for brain metastases in a cohort of patients with long-term follow up. 271 brain metastases treated with single-fraction linear accelerator-based SRS were analyzed. Radionecrosis was diagnosed either pathologically or radiographically. Univariate and multivariate Cox regression was performed to determine the association between radionecrosis and clinical factors available prior to treatment planning. After median follow up of 17.2 months, radionecrosis was observed in 70 (25.8 %) lesions, including 47 (17.3 %) symptomatic cases. 22 of 70 cases (31.4 %) were diagnosed pathologically and 48 (68.6 %) were diagnosed radiographically. The actuarial incidence of radionecrosis was 5.2 % at 6 months, 17.2 % at 12 months and 34.0 % at 24 months. On univariate analysis, radionecrosis was associated with maximum tumor diameter (HR 3.55, $p < 0.001$), prior whole brain radiotherapy (HR 2.21, $p = 0.004$), prescription dose (HR 0.56, $p = 0.02$)

Correspondence to: Kathryn Beal, bealk@mskcc.org.

Electronic supplementary material

The online version of this article (doi:10.1007/s11060-015-1881-3) contains supplementary material, which is available to authorized users.

Conflicts of Interest

The authors declare that they have no conflicts of interest.

and histology other than non-small cell lung, breast or melanoma (HR 1.85, p = 0.04). On multivariate analysis, only maximum tumor diameter (HR 3.10, p < 0.001) was associated with radionecrosis risk. This data demonstrates that with close imaging follow-up, radionecrosis after single-fraction SRS for brain metastases is not uncommon. Maximum tumor diameter on pre-treatment MR imaging can provide a reliable estimate of radionecrosis risk prior to treatment planning, with the greatest risk among tumors measuring >1 cm.

Keywords

SRS; Radiosurgery; Necrosis; Radionecrosis; Brain; Metastasis

Introduction

Stereotactic radiosurgery (SRS) is a widely utilized technique for the treatment of brain metastases. While SRS is generally well tolerated, a proportion of patients experience late treatment-related changes characteristic of radionecrosis. As most stringently defined, cerebral radionecrosis requires histologic demonstration of necrotizing alterations attributable to therapy involving native neuroparenchyma rather than, or in addition to, the target tumor. Characteristic features include hypocellular zones of necrosis and fibrinous exudates reflecting vascular injury, the latter also evidenced by vascular ectasia as well as hyalinizing and fibrinoid mural alterations of regional blood vessels. Dystrophic calcifications are commonly associated with this process, with inflammatory responses being quite variable. Because pathologic confirmation is not always possible, the diagnosis of radionecrosis is most commonly made on the basis of clinical symptoms and radiographic findings. In some cases, radionecrosis can cause neurologic symptoms requiring treatment with long-term steroids or surgical resection, while in other cases it can be entirely asymptomatic. When symptoms are not present, radionecrosis must be inferred based on the evolution of imaging changes over time and can be difficult to distinguish from other processes such as post-treatment inflammation. Reported rates of radionecrosis range from 2 % to greater than 30 % [1–8], but there remains a paucity of data on the actuarial rates of necrosis and related imaging changes with long-term follow up.

Several previous studies have attempted to investigate which factors are associated with the development of radionecrosis after SRS [3–6, 9–13], but the indications for SRS in these studies vary quite widely, with several including benign lesions such as arteriovenous malformations, which are typically treated with lower doses than metastatic lesions [9–13]. In addition, as several of these reports focus almost exclusively on treatment-related variables, the significance of patient and tumor characteristics prior to treatment planning has been incompletely characterized.

In this large, retrospective, single-institution study, we investigated the rate of radionecrosis, including pathologically confirmed or symptomatic radionecrosis and asymptomatic radiographic changes consistent with radionecrosis, in a closely-followed patient cohort treated for brain metastases using linear accelerator-based SRS. We also analyzed the association of radionecrosis with various clinical variables, with the goal of identifying

which pre-treatment characteristics could guide clinicians in estimating a patient's risk of radionecrosis prior to initiation of treatment planning.

Materials and methods

We retrospectively reviewed patients treated with single-fraction SRS for brain metastases at our institution from 2007 through 2009. Patients surviving fewer than 6 months after radiosurgery were excluded, as were lesions that had been surgically resected prior to SRS. Only lesions that were surgically resected after SRS, or followed for at least 6 months with MRI imaging after SRS were included in the final analysis.

Brain metastases were treated with linear accelerator-based SRS using a framed technique. Patients were immobilized in a Brown–Roberts–Wells (BRW) frame (Integra Radionics, Burlington, MA) and positioned using a localizing frame. The gross tumor volume (GTV) was determined with fused MR imaging. The planning target volume (PTV) was defined as a 2 mm three-dimensional expansion around the GTV. Radiation treatment plans consisted of 8–12 non-coplanar static fields using the micro-multileaf collimator m3 (BrainLAB, Feldkirchen, Germany). Plans were developed so that the 80 % isodose line (IDL) encompassed the PTV in the most conformal manner possible. The prescription dose, which was at the discretion of the treating physician, was prescribed to the 80 % IDL. In general, PTVs measuring less than 2 cm in greatest diameter were treated to 21 Gy, with smaller tumors occasionally receiving up to 22 Gy. PTVs measuring 2–3 cm were typically treated to 18 Gy, and PTVs greater than 3 cm were treated to 15 Gy. After the completion of SRS, patients were evaluated with a brain MRI at 2 months and every 3 months thereafter.

In patients undergoing post-SRS surgical resection, the presence of radionecrosis was determined based on histologic findings. For those patients without a pathologic diagnosis, radionecrosis was diagnosed if patients had MRI changes consistent with necrosis in the setting of new neurologic symptoms or a new steroid requirement. In asymptomatic patients, the diagnosis of radionecrosis was based on MRI (including diffusion-weighted imaging, perfusion-weighted imaging and MR spectroscopy) and FDG-PET. Treatment change consistent with radionecrosis was diagnosed if patients had either two consecutive MRIs with evidence of necrosis [14] or MRI accompanied by advanced MRI and/or PET imaging suggestive of necrosis [15–19]. Lesions with only one MRI demonstrating radionecrosis were carefully reviewed by the authors in the context of the overall clinical scenario. Lesions were scored as having radionecrosis if the MRI lacked evidence of distant intracranial progression and contained hallmark characteristics of necrosis including central hypodensity and peripheral enhancement on T1-weighted post-contrast imaging, with edema on T2-weighted sequences.

Actuarial incidence of radionecrosis was estimated using the Kaplan–Meier method, with lesions censored at time of resection or last brain MRI. If whole brain radiotherapy (WBRT) was delivered after SRS, lesions were not censored at the time of WBRT, in order to fully characterize all radionecrosis events observed in clinical practice. Cumulative incidence of radionecrosis requiring surgery was estimated using competing risks analysis, using death or surgery without radionecrosis as competing risks. Univariate Cox regression was performed

to investigate the relationship of radionecrosis with the following clinical factors: gender, age, Karnofsky performance status (KPS), tumor histology, tumor location, tumor size, prescription dose, prior WBRT, and use of concurrent cytotoxic chemotherapy or bevacizumab. Tumor size was recorded as the maximum diameter on pre-treatment MRI. Concurrent use of cytotoxic chemotherapy or bevacizumab was defined as administration within 8 weeks of SRS. Continuous variables were analyzed dichotomously, with the median value as a cutoff. For discrete variables with more than two groups, the largest group was used as the reference. Those factors with a p value of <0.10 on univariate analysis (UVA) were included in the multivariate analysis (MVA). Statistical significance was defined as a p value <0.05.

Results

We reviewed 327 patients with 583 metastatic lesions who received single-fraction SRS at our institution from 2007 to 2009. 160 patients with 271 lesions met the inclusion criteria. Median follow-up was 17.2 months (range 1.7–67.9). Patient and tumor characteristics at the time of SRS are listed in Table 1. The median patient age was 61 years (range 21–84). Patient KPS at the time of SRS was 90 % or greater in the majority of cases (65.1 %). Tumors were most commonly of non-small cell lung origin (42.8 %), with melanoma (22.9 %) and breast (15.9 %) the next most common. The median tumor size, as measured by maximum diameter of the GTV on MRI, was 1.1 cm (range 0.2–4.5). The median prescription dose was 21 Gy (range 15–22), with 74.9 % of lesions receiving a dose of 21 or 22 Gy. 39 lesions (14.4 %) had previously received WBRT.

Evidence of radionecrosis, including asymptomatic radiographic treatment change, was observed in 25.8 % (n = 70) of lesions. The actuarial incidence was 5.2 % at 6 months (95 % CI 2.5–7.8 %), 17.2 % at 12 months (95 % CI 12.1–22.0 %), 23.0 % at 18 months (95 % CI 17.0–28.6 %) and 34.0 % at 24 months (95 % CI 26.4–40.7 %) (Fig. 1). The median time to first diagnosis of radionecrosis was 10.7 months (range 2.7–47.7). Of those lesions that developed evidence of treatment change consistent with radionecrosis, 67.1 % (n = 47) were symptomatic (Table 2). The incidence of symptomatic radionecrosis was 11.8 % at 12 months (95 % CI 8.1–17.0 %)(Supplementary Fig. S1). The diagnosis of radionecrosis was confirmed pathologically in 22 (31.4 %) cases, with the remainder being diagnosed by imaging alone. Among those cases diagnosed by imaging, 27 were seen on MRI alone, while 21 were confirmed using FDG-PET imaging. 36 lesions were resected during the follow up period, either because of worsening neurologic symptoms or suspicion for disease progression. 22 of these were found to have evidence of radionecrosis. The cumulative incidence of radionecrosis requiring surgical resection was 5.5 % at 12 months (95 % CI 2.8–8.3 %)(Supplementary Fig. S2).

On UVA, radionecrosis, including asymptomatic treatment change, was associated with maximum tumor diameter (HR 3.55, 95 % CI 2.03–6.21, p < 0.001), prior WBRT (HR 2.21, 95 % CI 1.28–3.83, p = 0.004), prescription dose (HR 0.56, 95 % CI 0.34–0.91, p = 0.02) and histology other than non-small cell lung cancer, breast cancer or melanoma (HR 1.85, 95 % CI 1.02–3.37, p = 0.04) (Table 3). Multivariate regression revealed only tumor size (HR 3.10, 95 % CI 1.71–5.64, p < 0.001) to be significant. The grouping of “other”

histologic subtype nearly reached significance (HR 1.80, 95 % CI 0.98–3.33, p = 0.06). The highest rate of radionecrosis was observed among thyroid, ovarian and small cell lung cancer (Supplementary Table S1). When including only those lesions that were symptomatic or required surgery, radionecrosis remained significantly associated with maximum tumor diameter, prior WBRT and "other" histologic subtype on MVA (Supplementary Table S2).

Given the strong association between radionecrosis and maximum tumor diameter, the risk of radionecrosis was estimated based on this variable alone. The incidence of radionecrosis, including asymptomatic treatment change, was 2.9 % at 12 months in tumors measuring 0.5 cm or less (95 % CI 0.4–18.6 %), 6.6 % in tumors measuring 0.6–1.0 cm (95 % CI 2.8–13.1 %), 19.1 % in tumors measuring 1.1–1.5 cm (95 % CI 11.7–30.4 %) and 37.8 % in tumors measuring larger than 1.5 cm in greatest diameter (95 % CI 25.9–52.8 %) (Fig. 2). The incidence of symptomatic radionecrosis followed this same trend, with the lowest rates of radionecrosis seen in those tumors with a maximum diameter of 0.5 cm or less (Supplementary Fig. S3). Radionecrosis requiring surgery was rare in small tumors, with only one event occurring in lesions measuring 1.0 cm or less in maximum diameter.

Discussion

The estimated rate of radionecrosis after single-fraction SRS for brain metastases varies widely among studies. Previous large, prospective, multi-institutional trials investigating the effectiveness of SRS in treating brain metastases reported a low cumulative incidence of radionecrosis, on the order of 1.5–3.0 % [1, 2]. These studies were not designed to robustly evaluate for the development of symptomatic radionecrosis and did not record asymptomatic treatment change. Multiple retrospective studies have reported higher rates of radionecrosis, ranging from 6.2 % to more than 30 % [3–7], likely reflecting differences in patient population, extent of follow up, and definition of radionecrosis.

We report a crude rate of radionecrosis, including both symptomatic and asymptomatic treatment change, of 25.8 %. This is toward the upper range of other similar retrospective studies. Several potential explanations may exist. First, all patients included in this study were followed closely with imaging, including brain MRIs every 3 months and FDG-PET scans as needed to help distinguish necrosis from recurrence. This intensive follow up allowed us to capture events that may have been missed if patients had been lost to follow up or incompletely imaged. In addition, unlike some other studies, we chose to exclude those patients who survived fewer than 6 months [3, 5]. Because the diagnosis of radionecrosis typically requires multiple imaging studies over time, excluding lesions with short follow up likely increased our event rate. Furthermore, detection of radionecrosis may have been increased due to the high frequency of surgical resection in our cohort. This high rate of post-SRS resection provides a definitive diagnosis of necrosis in some cases that may otherwise have been thought to represent disease progression. In support of this, we report pathologic confirmation of radionecrosis in 31.4 % of cases (Table 2), while other series examining radionecrosis rates report pathologic confirmation in only 0–25 % of cases [4–6].

In addition to investigating the rate of radionecrosis, we also sought to determine which clinical factors were associated with the development of radionecrosis. Maximum tumor

diameter on pre-SRS MRI was most strongly associated with radionecrosis, on both UVA and MVA (Table 3). Even when asymptomatic radionecrosis was excluded from the analysis, maximum tumor diameter remained strongly significant (Supplementary Table S2). While tumor volume has previously been identified as a predictor of SRS complications [12, 20, 21] and radionecrosis after SRS [8, 10, 22], many of these studies included hetereogenous treatment indications and populations. Our data add to the literature by clearly defining maximum tumor diameter as the most important pretreatment clinical factor determining necrosis risk in patients undergoing single-fraction linear accelerator-based SRS for brain metastases (Fig. 2).

It is important to note that multiple prior studies have reported relationships between dose-volume parameters and radionecrosis risk–first in the setting of arteriovenous malformation (AVM) [9, 23, 24] and subsequently in brain tumors treated with SRS [25]. Multiple dose-volume parameters have been suggested to associate with radionecrosis risk, including V10 Gy [11, 26], V12 Gy [3, 6], V10–V18 Gy [5], V8–V18 Gy [4], V15 Gy [6] and V22 Gy [6]. While these studies have been important in developing our understanding of radionecrosis and its underlying causes, differences in technique and inclusion criteria between these studies have precluded implementation of a single widely applicable dose-volume parameter. Furthermore, treatment planning variables are unavailable to clinicians at the time of consultation, when initial decisions must be made regarding the relative risks and benefits of radiosurgery for a given patient. In order to guide clinical decision-making at the time of initial consultation, we chose not to include dose-volume parameters in our analysis, instead limiting our study to variables known prior to initiation of treatment planning.

Aside from tumor size, “other” tumor histology nearly reached significance on MVA. This is a grouping comprised of twelve uncommon histologic subtypes excluding melanoma, breast carcinoma and non-small cell lung carcinoma. The high rate of necrosis in this group was driven by the relatively large number of events in tumors of thyroid, ovarian, and small cell lung histology (Supplementary Table S1). While possible explanations may exist, such as increased use of WBRT in patients with small cell lung cancer, the small number of patients with these tumor types in our study precludes any further analysis.

Bevacizumab has been reported to be effective in treating radionecrosis [27, 28]. We included use of this agent in our analysis to determine if it is protective against radionecrosis. We did not observe a decreased risk of radionecrosis, perhaps because only 24 lesions received bevacizumab concurrent with SRS treatment.

Prior WBRT was associated with an increased risk for radionecrosis on UVA. When considering only symptomatic lesions or those requiring surgery, prior WBRT retained significance on MVA. The suggestion that WBRT may predispose patients to the development of radionecrosis is supported by Korytko et al., who found an association between symptomatic radionecrosis and prior WBRT in metastatic and primary brain tumors treated with SRS [3]. Our data suggests that caution should be used when treating previously irradiated brain metastases with single-fraction SRS, particularly in patients with large lesions or a relatively long expected survival time. While we had also intended to study the

contribution of post-SRS WBRT to radionecrosis rates, the short follow up after salvage WBRT in the majority of cases precluded this.

Low prescription dose (<21 Gy) was associated with a higher risk for radionecrosis. This association may be due to the larger average tumor size in the low dose group (1.8 vs. 0.9 cm), suggesting that the risk of radionecrosis associated with larger tumor size may outweigh any potential mitigating effect of a lower radiation dose. The prescribed doses in our patient cohort paralleled those used in RTOG 90-05, yet we observed higher overall rates of radionecrosis than were reported in that study [8]. The rate of radionecrosis requiring surgery in our study was comparable to that reported in RTOG 90-05 (5.5 vs. 8 % at 12 months). In contrast, we observed clinical or radiographic evidence of radionecrosis in 48 (17.7 %) lesions, as compared to only one (0.6 %) in RTOG 90-05. This may be explained by the less intensive radiographic follow up in RTOG 90-05. While we followed patients with brain MRIs every 3 months after SRS, patients enrolled in RTOG 90-05 could be followed by CT scans alone and were imaged only every 6 months after the first year. Notably, 27 % of patients in RTOG 90-05 required steroids at some time after SRS, perhaps representing a subset of patients with unrecognized radionecrosis that may have been evident with more intensive follow up. We posit that our findings are not incongruous with those reported in RTOG 90-05. Rather, our results suggest that with routine MR imaging and close clinical follow up, radionecrosis is more readily identified.

A significant limitation of our study and others remains the inadequacy of current imaging techniques to distinguish between necrosis and tumor. While advanced imaging studies such as FDG-PET may add diagnostic accuracy and were often utilized in our patient cohort, the sensitivity and specificity of such techniques are suboptimal [29, 30]. Future studies should be aimed at correlating imaging findings with pathologic diagnoses, to determine whether a reliable imaging signature for necrosis can be defined. We are currently investigating other imaging modalities such as 18F-fluorocholine PET imaging, in an effort to identify better ways to distinguish necrosis from tumor progression [31].

In conclusion, we demonstrate that radionecrosis rates steadily increase over time after SRS. Although our reported rates are higher than in some other series, we believe this reflects the close follow up of our patient cohort with frequent MR imaging, which is a strength of our study. Furthermore, our rates of radionecrosis include not only symptomatic or pathologically confirmed necrosis, but also asymptomatic imaging changes from which a diagnosis of necrosis can be reasonably inferred. We demonstrate that the risk of radionecrosis strongly correlates with maximum tumor diameter on brain MRI. Such a correlation is clinically very useful, as tumor diameter can be used to assess radionecrosis risk prior to initiation of SRS planning. Given that radionecrosis is not always symptomatic, and tumor control is often difficult to achieve in larger tumors, we have not lowered our radiosurgery doses based on this data. As patient survival continues to improve in the metastatic setting, however, balancing tumor control and late complications such as radionecrosis will be increasingly important. Together, our data provides a thorough characterization of the rate of radionecrosis after SRS in patients with intensive follow up treated with modern radiotherapy techniques for brain metastases.

Supplementary Material

Refer to Web version on PubMed Central for supplementary material.

References

1. Kocher M, Soffietti R, Abacioglu U, Villa S, Fauchon F, Baumert BG, Fariselli L, Tzuk-Shina T, Kortmann RD, Carrie C, Ben Hassel M, Kouri M, Valeinis E, van den Berge D, Collette S, Collette L, Mueller RP. Adjuvant whole-brain radiotherapy versus observation after radiosurgery or surgical resection of one to three cerebral metastases: results of the EORTC 22952-26001 study. J Clin Oncol. 2011; 29:134–141.10.1200/JCO.2010.30.1655 [PubMed: 21041710]
2. Aoyama H, Shirato H, Tago M, Nakagawa K, Toyoda T, Hatano K, Kenjyo M, Oya N, Hirota S, Shioura H, Kunieda E, Inomata T, Hayakawa K, Katoh N, Kobashi G. Stereotactic radiosurgery plus whole-brain radiation therapy vs stereotactic radiosurgery alone for treatment of brain metastases: a randomized controlled trial. JAMA, J Am Med Assoc. 2006; 295:2483–2491.10.1001/jama.295.21.2483
3. Korytko T, Radivoyevitch T, Colussi V, Wessels BW, Pillai K, Maciunas RJ, Einstein DB. 12 Gy gamma knife radiosurgical volume is a predictor for radiation necrosis in non-AVM intracranial tumors. Int J Radiat Oncol Biol Phys. 2006; 64:419–424.10.1016/j.ijrobp.2005.07.980 [PubMed: 16226848]
4. Blonigen BJ, Steinmetz RD, Levin L, Lamba MA, Warnick RE, Breneman JC. Irradiated volume as a predictor of brain radionecrosis after linear accelerator stereotactic radiosurgery. Int J Radiat Oncol Biol Phys. 2010; 77:996–1001.10.1016/j.ijrobp.2009.06.006 [PubMed: 19783374]
5. Minniti G, Clarke E, Lanzetta G, Osti MF, Trasimeni G, Bozzao A, Romano A, Enrici RM. Stereotactic radiosurgery for brain metastases: analysis of outcome and risk of brain radionecrosis. Radiat Oncol. 2011; 6:48.10.1186/1748-717X-6-48 [PubMed: 21575163]
6. Ohtakara K, Hayashi S, Nakayama N, Ohe N, Yano H, Iwama T, Hoshi H. Significance of target location relative to the depth from the brain surface and high-dose irradiated volume in the development of brain radionecrosis after micromultileaf collimator-based stereotactic radiosurgery for brain metastases. J Neurooncol. 2012; 108:201–209.10.1007/s11060-012-0834-3 [PubMed: 22392126]
7. Schuttrumpf LH, Niyazi M, Nachbichler SB, Manapov F, Jansen N, Siefert A, Belka C. Prognostic factors for survival and radiation necrosis after stereotactic radiosurgery alone or in combination with whole brain radiation therapy for 1–3 cerebral metastases. Radiat Oncol. 2014; 9:105.10.1186/1748-717X-9-105 [PubMed: 24885624]
8. Shaw E, Scott C, Souhami L, Dinapoli R, Kline R, Loeffler J, Farnan N. Single dose radiosurgical treatment of recurrent previously irradiated primary brain tumors and brain metastases: final report of RTOG protocol 90-05. Int J Radiat Oncol Biol Phys. 2000; 47:291–298. [PubMed: 10802351]
9. Flickinger JC, Kondziolka D, Pollock BE, Maitz AH, Lunsford LD. Complications from arteriovenous malformation radiosurgery: multivariate analysis and risk modeling. Int J Radiat Oncol Biol Phys. 1997; 38:485–490. [PubMed: 9231670]
10. Miyawaki L, Dowd C, Wara W, Goldsmith B, Albright N, Gutin P, Halbach V, Hieshima G, Higashida R, Lulu B, Pitts L, Schell M, Smith V, Weaver K, Wilson C, Larson D. Five year results of LINAC radiosurgery for arteriovenous malformations: outcome for large AVMS. Int J Radiat Oncol Biol Phys. 1999; 44:1089–1106. [PubMed: 10421543]
11. Voges J, Treuer H, Sturm V, Buchner C, Lehrke R, Kocher M, Staar S, Kuchta J, Muller RP. Risk analysis of linear accelerator radiosurgery. Int J Radiat Oncol Biol Phys. 1996; 36:1055–1063. [PubMed: 8985027]
12. Nakamura JL, Verhey LJ, Smith V, Petti PL, Lamborn KR, Larson DA, Wara WM, McDermott MW, Sneed PK. Dose conformity of gamma knife radiosurgery and risk factors for complications. Int J Radiat Oncol Biol Phys. 2001; 51:1313–1319. [PubMed: 11728692]
13. Barker FG 2nd, Butler WE, Lyons S, Cascio E, Ogilvy CS, Loeffler JS, Chapman PH. Dose-volume prediction of radiation-related complications after proton beam radiosurgery for cerebral

arteriovenous malformations. J Neurosurg. 2003; 99:254–263.10.3171/jns.2003.99.2.0254 [PubMed: 12924697]

14. Mullins ME, Barest GD, Schaefer PW, Hochberg FH, Gonzalez RG, Lev MH. Radiation necrosis versus glioma recurrence: conventional MR imaging clues to diagnosis. AJNR Am J Neuroradiol. 2005; 26:1967–1972. [PubMed: 16155144]
15. Fatterpekar GM, Galheigo D, Narayana A, Johnson G, Knopp E. Treatment-related change versus tumor recurrence in high-grade gliomas: a diagnostic conundrum–use of dynamic susceptibility contrast-enhanced (DSC) perfusion MRI. AJR Am J Roentgenol. 2012; 198:19–26.10.2214/AJR.11.7417 [PubMed: 22194475]
16. Barajas RF, Chang JS, Sneed PK, Segal MR, McDermott MW, Cha S. Distinguishing recurrent intra-axial metastatic tumor from radiation necrosis following gamma knife radiosurgery using dynamic susceptibility-weighted contrast-enhanced perfusion MR imaging. AJNR Am J Neuroradiol. 2009; 30:367–372.10.3174/ajnr.A1362 [PubMed: 19022867]
17. Gasparetto EL, Pawlak MA, Patel SH, Huse J, Woo JH, Krejza J, Rosenfeld MR, O' Rourke DM, Lustig R, Melhem ER, Wolf RL. Posttreatment recurrence of malignant brain neoplasm: accuracy of relative cerebral blood volume fraction in discriminating low from high malignant histologic volume fraction. Radiology. 2009; 250:887–896.10.1148/radiol.2502071444 [PubMed: 19244052]
18. Enslow MS, Zollinger LV, Morton KA, Butterfield RI, Kadrmas DJ, Christian PE, Boucher KM, Heilbrun ME, Jensen RL, Hoffman JM. Comparison of 18F-fluorodeoxyglucose and 18F-fluorothymidine PET in differentiating radiation necrosis from recurrent glioma. Clin Nucl Med. 2012; 37:854–861.10.1097/RLU.0b013e318262c76a [PubMed: 22889774]
19. Hatzoglou V, Ulaner GA, Zhang Z, Beal K, Holodny AI, Young RJ. Comparison of the effectiveness of MRI perfusion and fluorine-18 FDG PET-CT for differentiating radiation injury from viable brain tumor: a preliminary retrospective analysis with pathologic correlation in all patients. Clin Imaging. 2013; 37:451–457.10.1016/j.clinimag.2012.08.008 [PubMed: 23068052]
20. Nedzi LA, Kooy H, Alexander E 3rd, Gelman RS, Loeffler JS. Variables associated with the development of complications from radiosurgery of intracranial tumors. Int J Radiat Oncol Biol Phys. 1991; 21:591–599. [PubMed: 1907957]
21. Varlotto JM, Flickinger JC, Niranjan A, Bhatnagar AK, Kondziolka D, Lunsford LD. Analysis of tumor control and toxicity in patients who have survived at least one year after radiosurgery for brain metastases. Int J Radiat Oncol Biol Phys. 2003; 57:452–464. [PubMed: 12957257]
22. Varlotto JM, Flickinger JC, Niranjan A, Bhatnagar A, Kondziolka D, Lunsford LD. The impact of whole-brain radiation therapy on the long-term control and morbidity of patients surviving more than one year after gamma knife radiosurgery for brain metastases. Int J Radiat Oncol Biol Phys. 2005; 62:1125–1132.10.1016/j.ijrobp.2004.12.092 [PubMed: 15990018]
23. Kjellberg RN, Hanamura T, Davis KR, Lyons SL, Adams RD. Bragg-peak proton-beam therapy for arteriovenous malformations of the brain. N Engl J Med. 1983; 309:269–274.10.1056/NEJM198308043090503 [PubMed: 6306463]
24. Flickinger JC, Lunsford LD, Kondziolka D, Maitz AH, Epstein AH, Simons SR, Wu A. Radiosurgery and brain tolerance: an analysis of neurodiagnostic imaging changes after gamma knife radiosurgery for arteriovenous malformations. Int J Radiat Oncol Biol Phys. 1992; 23:19–26. [PubMed: 1572817]
25. Lawrence YR, Li XA, el Naqa I, Hahn CA, Marks LB, Merchant TE, Dicker AP. Radiation dose-volume effects in the brain. Int J Radiat Oncol Biol Phys. 2010; 76:S20–S27.10.1016/j.ijrobp.2009.02.091 [PubMed: 20171513]
26. Chin LS, Ma L, DiBiase S. Radiation necrosis following gamma knife surgery: a case-controlled comparison of treatment parameters and long-term clinical follow up. J Neurosurg. 2001; 94:899–904.10.3171/jns.2001.94.6.0899 [PubMed: 11409517]
27. Boothe D, Young R, Yamada Y, Prager A, Chan T, Beal K. Bevacizumab as a treatment for radiation necrosis of brain metastases post stereotactic radiosurgery. Neuro-oncology. 2013; 15:1257–1263.10.1093/neuonc/not085 [PubMed: 23814264]
28. Levin VA, Bidaut L, Hou P, Kumar AJ, Wefel JS, Bekele BN, Grewal J, Prabhu S, Loghin M, Gilbert MR, Jackson EF. Randomized double-blind placebo-controlled trial of bevacizumab therapy for radiation necrosis of the central nervous system. Int J Radiat Oncol Biol Phys. 2011; 79:1487–1495.10.1016/j.ijrobp.2009.12.061 [PubMed: 20399573]

29. Belohlavek O, Simonova G, Kantorova I, Novotny J Jr, Liscak R. Brain metastases after stereotactic radiosurgery using the Leksell gamma knife: can FDG PET help to differentiate radionecrosis from tumour progression? Eur J Nucl Med Mol Imaging. 2003; 30:96–100.10.1007/s00259-002-1011-2 [PubMed: 12483415]

30. Langleben DD, Segall GM. PET in differentiation of recurrent brain tumor from radiation injury. J Nucl Med. 2000; 41:1861–1867. [PubMed: 11079496]

31. Memorial Sloan-Kettering Cancer Center; National Institutes of Health. ClinicalTrials.gov [Internet]. Bethesda (MD): National Library of Medicine (US); 2000. 18F-Fluorocholine (18F-FCho) to Distinguish Necrosis From Recurrence in Brain Metastases. [cited 2014 Oct 26]. Available from: https://clinicaltrials.gov/ct2/show/NCT02037945. NLM Identifier: NCT02037945

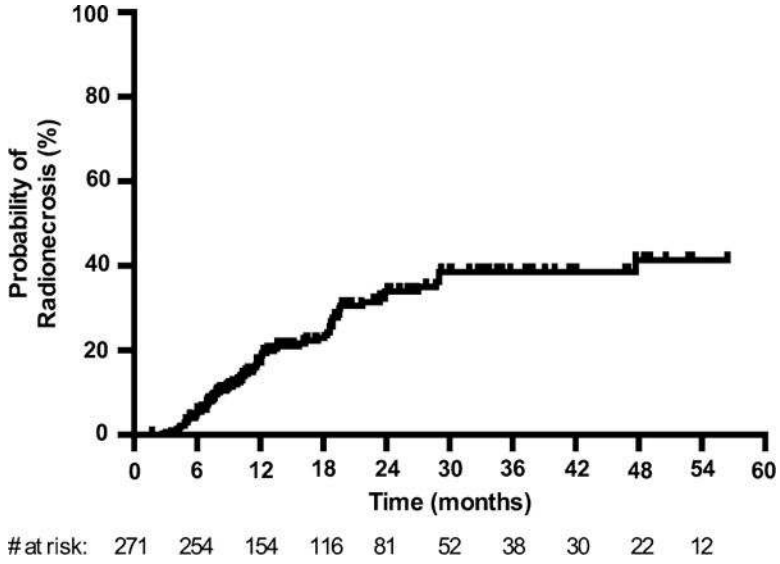

Fig. 1.
Actuarial incidence of radionecrosis

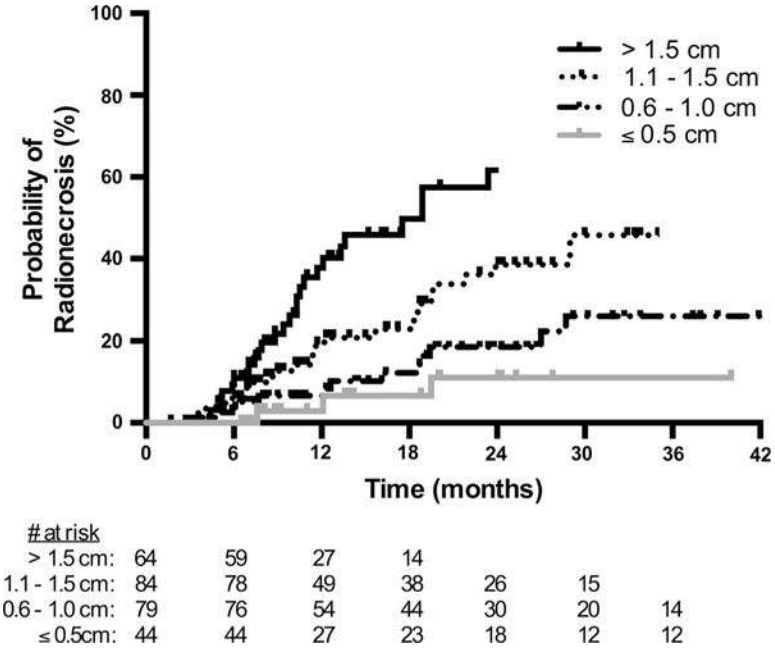

# at risk							
> 1.5 cm:	64	59	27	14			
1.1 - 1.5 cm:	84	78	49	38	26	15	
0.6 - 1.0 cm:	79	76	54	44	30	20	14
≤ 0.5cm:	44	44	27	23	18	12	12

Fig. 2.

Actuarial incidence of radionecrosis, stratified by maximum tumor diameter of ≤0.5, 0.6–1.0, 1.1–1.5, and >1.5 cm

Table 1

Summary of patient, tumor and treatment characteristics

Patient characteristics at time of SRS	
Age (years), median (range)	61 (21–84)
KPS (%), median (range)	90 (70–100)
Gender	
Female	106 (66.3 %)
Male	54 (33.7 %)
Tumor characteristics	
Maximum tumor diameter (cm)	
≤1.0	123 (45.4 %)
>1.0	148 (54.6 %)
Location	
Frontal/parietal	157 (57.9 %)
Temporal/occipital	49 (18.1 %)
Cerebellar	55 (20.3 %)
Other	10 (3.7 %)
Histology	
NSCLC	116 (42.8 %)
Melanoma	62 (22.9 %)
Breast	43 (15.9 %)
Other	50 (18.4 %)
Treatment characteristics	
Dose (Gy)	
<21	68 (25.1 %)
≥21	203 (74.9 %)
Prior WBRT	
Yes	39 (14.4 %)
No	232 (85.6 %)
Concurrent chemotherapy	
Yes	120 (44.3 %)
No	151 (55.7 %)
Concurrent bevacizumab	
Yes	24 (8.9 %)
No	247 (91.1 %)

Table 2

Characteristics of radionecrosis diagnosis

Necrosis characteristics	Number (%) of lesions
Time to necrosis (months), median (range)	10.8 (2.7–47.7)
Presence of symptoms	
Yes	47 (67.1 %)
No	23 (32.9 %)
Method of diagnosis	
Pathologic	22 (31.4 %)
Radiographic	48 (68.6 %)
MRI alone	27 (38.6 %)
MRI with PET	21 (30.0 %)

Table 3

Univariate and multivariate analysis of clinical factors potentially prognostic for radionecrosis

	Actuarial incidence (%)		Univariate analysis		Multivariate analysis	
	12 months	**24 months**	**Hazard ratio (95 % CI)**	**p Value**	**Hazard ratio (95 % CI)**	**p Value**
Age (years)						
≤60	14.9	34.2	1.10 (0.67–1.83)	0.70		
>60	19.3	33.8				
KPS (%)						
70–80	23.0	27.3	1.15 (0.69–1.90)	0.59		
90–100	14.4	37.5				
Gender						
Male	15.0	29.6	0.81 (0.45–1.43)	0.46		
Female	17.9	35.1				
Maximum tumor diameter (cm)						
≤1.0	5.2	16.0	3.55 (2.03–6.21)	<0.001**	3.10 (1.71–5.64)	<0.001**
>1.0	26.9	49.4				
Location						
Frontal/parietal	15.7	34.3	Reference	N/A		
Temporal/occipital	29.4	37.5	1.34 (0.72–2.52)	0.36		
Cerebellar	10.2	30.2	0.95 (0.52–1.75)	0.87		
Other	27.1	27.1	0.84 (0.20–3.48)	0.81		
Histology						
NSCLC	17.5	31.5	Reference	N/A	Reference	N/A
Melanoma	9.1	23.6	0.65 (0.30–1.41)	0.27	0.79 (0.36–1.77)	0.57
Breast	13.5	35.9	1.27 (0.68–2.36)	0.46	1.08 (0.54–2.13)	0.83
Other	29.0	56.4	1.85 (1.02–3.37)	0.04*	1.80 (0.98–3.33)	0.06
Dose (Gy)						
<21	27.9	45.6	0.56 (0.34–0.91)	0.02*	0.93 (0.54–1.59)	0.78
≥21	13.6	30.0				
Prior WBRT						
Yes	25.1	49.9	2.21 (1.28–3.83)	0.004**	1.54 (0.83–2.86)	0.17

	Actuarial incidence (%)		Univariate analysis		Multivariate analysis	
	12 months	24 months	Hazard ratio (95 % CI)	p Value	Hazard ratio (95 % CI)	p Value
No	15.9	31.1				
Concurrent chemotherapy						
Yes	10.1	35.6	0.81 (0.50–1.33)	0.41		
No	23.0	34.1				
Concurrent bevacizumab						
Yes	0	31.8	0.57 (0.21–1.56)	0.27		
No	19.0	34.5				

* p value <0.05

** p value <0.01